

Central European Journal of Engineering

Experimental and Numerical Investigation of Slabs on Ground Subjected to Concentrated Loads

Research Article

Jan Øverli1*

1 Department of Structural Engineering, Norwegian University of Science and Technology NO-7004 Trondheim, Norway

Received 25 July 2013; accepted 26 February 2014

Abstract: An experimental program is presented where a slab on ground is subjected to concentrated loading at the centre, the edges and at the corners. Analytical solutions for the ultimate load capacity fit well with the results obtained in the tests. The non-linear behaviour of the slab is captured by performing nonlinear finite element analyses. The soil is modelled as a no-tension bedding and a smeared crack approach is employed for the concrete. Through a parametric study, the finite element model has been used to assess the influence of subgrade stiffness and shrinkage. The results indicate that drying shrinkage can cause severe cracking in slabs on grade.

Keywords: Slabs on ground • Concentrated load • Experiment • Numerical • Cracking • Failure • Shrinkage • Subgrade stiffness

© Versita sp. z o.o.

Introduction 1.

Slabs on ground are often subjected to demanding service conditions. For industrial slabs and floors in buildings the owner and the builder often require crack free surfaces. Hence, in addition to have enough load capacity, it is important to keep control of cracking and crack widths. Typical loading which influence both serviceability and load capacity are concentrated loads from vehicles, columns or leg loads from storage platforms.

From a structural point, slabs on ground are large planes lying on continuous support. The maximum bending moments are directly under the concentrated loads and introduce a radial crack pattern at the bottom of the slab. At higher load levels, circular cracks forms at

the top surface at some distance from the loaded area. The response of the slab depends on many factors, e.g. loaded area, slab size, subgrade stiffness. These have been extensively investigated experimentally [1, 2] and theoretically by many researchers [3-8]. The use of steel fibre in slabs on ground is widely used around the world. However, in the Scandinavian countries the majority of slabs are still produced with longitudinal reinforcement.

Design of slabs on ground are normally based on either elastic or plastic methods [9-11]. In situations where cracking is unacceptable elastic methods should be used while plastic methods could be used in slabs where controlled cracking is acceptable. According to elastic theory, the problem was solved for concentrated loading by Westgaard [3], when the loading was uniformly distributed over a small circular area. introduced the term modulus of subgrade reaction, which is the load per unit area causing unit deflection of the subgrade. This represents a Winkler foundation which

^{*}E-mail: Jan.Overli@ntnu.no

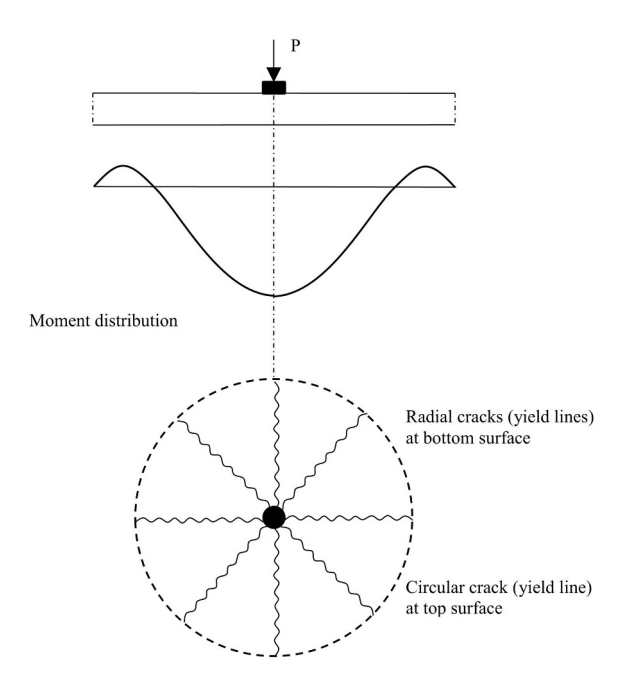


Figure 1. Distribution of bending moments and formation of cracks (yield lines).

assumes that reactions from the subgrade are vertical only and can be represented by vertical elastic springs.

At ultimate limit state (ULS) the resistance of slabs subjected to concentrated loading is governed by bending failure, bearing strength or punching failure. Bending capacity can be calculated by means of conventional yield line theory. Meyerhof developed design equations for concentrated internal, edge and corner loads [4]. The governing failure mechanism is cone-shaped with radial yield lines (from the loaded area) and a circular yield line forming some distance away from the loaded area, as illustrated in Figure 1. The collapse loads in bending are given as:

Internal load:

$$P_{i} = \frac{4\pi(M_{p} + M_{n})}{1 - \frac{a}{3 \cdot l}}, \quad \frac{a}{l} > 0.2$$

$$P_{u} = 2\pi(M_{p} + M_{n}), \quad \frac{a}{l} = 0$$
(1)

Edge load:

$$P_{u} = \frac{\pi(M_{p} + M_{n}) + 4M_{n}}{1 - \frac{2a}{3 \cdot l}}, \quad \frac{a}{l} > 0.2$$

$$P_{u} = \frac{\pi(M_{p} + M_{n})}{2} + 2M_{n}, \quad \frac{a}{l} = 0$$
(2)

Corner load:

$$P_{u} = 2\left(1 + \frac{4a}{l}\right) \cdot M_{n}, \quad \frac{a}{l} > 0.2$$

$$P_{u} = 2 \cdot M_{n}, \quad \frac{a}{l} = 0$$
(3)

where M_n and M_p are hogging and sagging moment resistance of the slab respectively, a the equivalent radius of the load and l the radius of relative stiffness. Linear interpolation can be used for values of a/l between 0 and 0.2. The radius of relative stiffness is defined as:

$$l = \sqrt[4]{\frac{E_c \cdot h^3}{12(1 - v^2) \cdot k}} \tag{4}$$

where E_c is modulus of elasticity of concrete, h the slab depth, ν Poisson's ratio and k the modulus of subgrade reaction. To avoid cracking at the upper surface, the hogging yield line should be limited to the design cracking moment.

Design codes often define the bearing capacity f_c^* as [12, 13]:

$$f_c^* = f_{cd} \sqrt{\frac{A_2}{A_1}} \tag{5}$$

where f_{cd} is the uniaxial compressive design strength, A_1 the partially loaded area and A_2 the distribution area. Limitations of the distribution area are introduced to take into account loads close to an edge, eccentric loading or overlapping loads. Punching resistance in Eurocode 2 (EC2) must be checked at the face of the concentrated load and at a critical perimeter a distance 2d (where d is the effective depth) from the loaded area. The shear stress resistance at the face of the loaded area is given as:

$$v_{max} = 0.4 \cdot \upsilon \cdot f_{cd} \tag{6}$$

where f_{cd} is the design compressive strength and $v=0.6(1-f_{ck}/250)$. In EC2, the shear stress carried by the concrete at the critical perimeter yields:

$$v_{Rd,c} = \frac{0.18}{\gamma_c} \cdot k \cdot (100\rho_l f_{ck})^{\frac{1}{3}} \tag{7}$$

where k takes into account the size effect and ρ_l the effect of the longitudinal reinforcement. Due to the support of the ground bearing slab, this design section is rarely critical.

This paper focuses on slabs subjected to concentrated loading. However, restraints to thermal and shrinkage

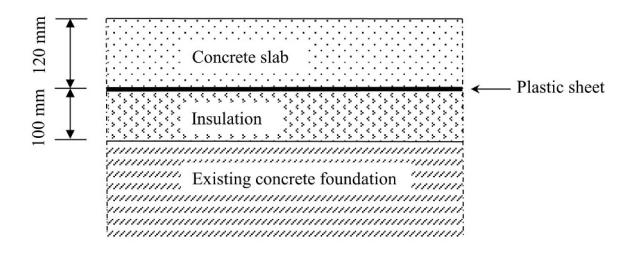


Figure 2. Cross-section of slab and subgrade.

movements can contribute significantly to the structural response of a ground bearing slab [14].

Aim of this study is to investigate slabs on ground subjected to concentrated loading. An experimental program is set up to find static capacities and to study the formation of cracks. Static load carrying capacities are compared to yield line solutions. Finally, non-linear finite element analyses are performed to validate the experimental results.

The experimental work has been carried out as part of a Master thesis project at the Department of Structural Engineering at Norwegian University of Science and Technology [15].

2. Experimental program and results

2.1. Experimental program

Ground slabs exposed to heavy truck loads often experience damage due to extensive cracking. Often this is a result of inadequate design. To study this in detail a test program was set up for a slab subjected to static concentrated loading, and measuring the deformation, strains and failure loads. The experimental program covers one slab. This slab was subjected to loading at the centre, at two edges and two corners. Due to the very locale response of a concentrated load, failure at one location in slab has only minor influence on the subsequent failure loads at the other locations. The slab had a square geometry with dimensions 3500×3500 mm. The thickness of the slab was 120 mm. A layer of 100 mm of insulation represented the supporting soil. A plastic sheet between the slab and insulation minimise the friction and moisture transportation. Figure 2 shows the cross-section of the slab and the subgrade.

The testing facilities in the laboratory limited the slab



Figure 3. Ground slab and test set-up [15].

size. However, to simulate a larger slab, three points along each edge of the slab were fixed against vertical deformation as shown in Figure 3. When applying the edge and the corner loads, the restraints close to the loading point were removed.

Depending on the soil type, the subgrade stiffness is typical in the range 0.01-0.5 N/mm³. Crushed stone which is often used as a subgrade has a stiffness of 0.15 N/mm³. To achieve this stiffness in the testing system, a 100 mm thick layer of Jackofoam 400 XPS was used. This is an insulation material made of extruded polystyrene, with a high compressive strength. Compressive test results on cubic polystyrene specimens with 100 mm sides, is given in Figure 4. By calculating the difference quotient between one and two mm displacement in the diagram, the average stiffness is approximately 0.15 N/mm³.

The loading area on the slab is 100×100 mm, representing a surface load since this study mainly focuses on the bending behaviour of the slab. A typical wheel load area is smaller and much more rectangular, but a larger quadratic load area was chosen to avoid a punching failure.

The slab is reinforced with orthogonal longitudinal reinforcement at both top and bottom with a concrete cover of 20 mm. This is a rather low value in practice for slabs on ground for durability reasons. However, in this experimental program it is sufficient. According to Eurocode 2 the required minimum reinforcement is given as:

$$A_{s,min} = 0.26 \cdot \frac{f_{ctm}}{f_{yk}} \cdot b_t \cdot d > 0.0013 \cdot b_t \cdot d \qquad (8)$$

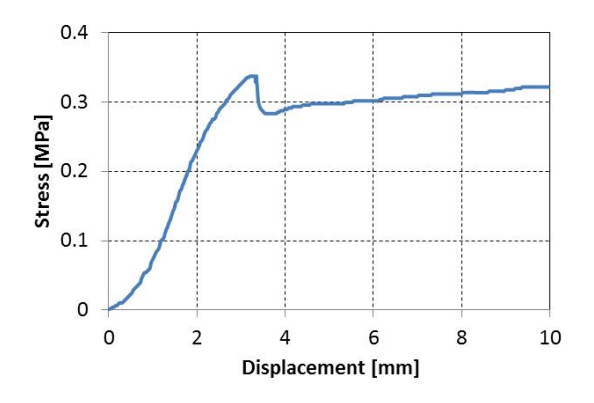


Figure 4. Compressive test of subgrade material.

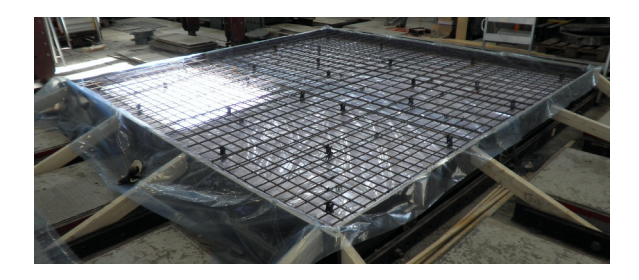


Figure 5. Casting frame and reinforcement arrangement [15].

where f_{ctm} is the mean tensile strength, f_{yk} is the characteristic yield strength of the reinforcement, b_t the width of the tensile zone and d the effective height of the cross-section. Assuming a concrete strength class of C30/37 and a yield stress for the reinforcement of 560 N/mm², the required minimum reinforcement is 129 mm²/m. To minimise crack widths in ground slabs, this value is often doubled. Hence, in this study reinforcement bars with diameter 8 mm and a distance between bars of 156 mm is used giving 322 mm²/m. The reinforcement arrangement and casting frame is illustrated in Figure 5. In order to control the mechanical properties, cylinders were casted to evaluate the compressive strength according to NS-EN 12390-3 [16] and the modulus of elasticity [17]. The mean values obtained after 28-day of curing was 32.1 N/mm² and 26727 N/mm², respectively. Keeping control of the cracking due to bending at the top surface is of great importance in design of concrete slabs on ground. Hence, the flexural tensile strength, $f_{ctm.fl}$, is an important parameter. To estimate the strength, six

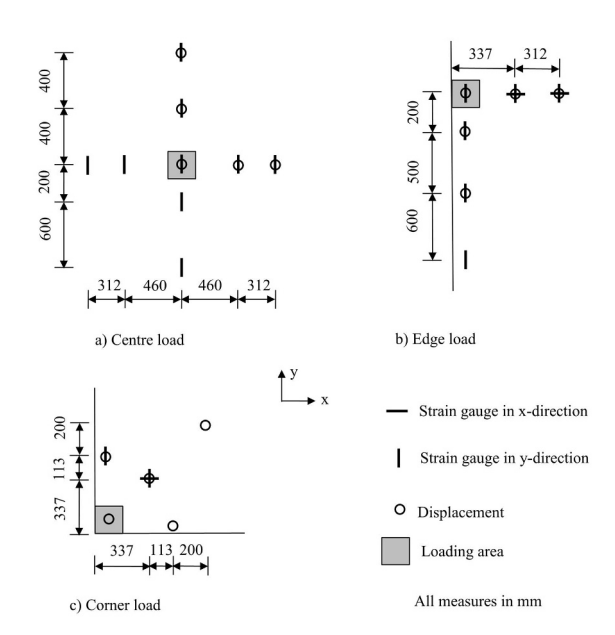


Figure 6. Location points for measurements.

simply supported unreinforced beams with cross section 100×100 mm and a span of 1000 mm were tested under 4 point bending with a load spacing of 200 mm. Based on the failure (cracking) loads in the experiment, the flexural tensile strength was $5.1\ N/mm^2$, with a relative standard deviation of 6%.

To capture the structural response of the slab, the deformation and strains must be measured. Figure 6 shows the location of the strain gauges and LVDT for displacements. Strain gauges were installed at both the top and bottom reinforcement at the measuring points. In total, 90 strain gauges were used. Location of the strain gauges was based on the result of linear elastic finite element analyses. At the bottom surface, the largest tensile stresses occur close to the loaded area. To fit with the reinforcement layout some adjustments of the location points were compared to the results from the analyses.

To apply the static loading, a hydraulic jack was used together with a control computer. To transfer the load from the hydraulic jack, a steel prism was used as the loading area, as seen in Figure 7. Between the jack and prism specimen, a ball-and-socket joint was placed to avoid bending moments in case of inclined loading. During testing the load was incremented with steps of 20 kN to allow for inspection and marking of cracks.

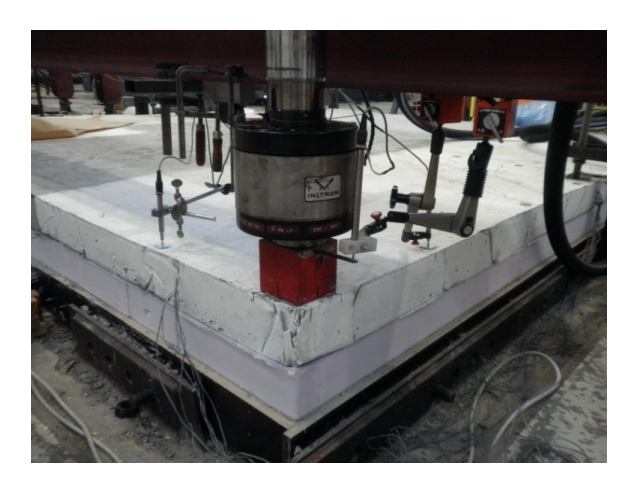


Figure 7. Test arrangement and load cell for corner load [15].

2.2. Experimental results

This section presents the results from the experimental program. The focus is on failure loads, deformation, crack development and circumferential strains around the loaded area at the top surface. A full description of all experimental results is given in [15]. The failure loads, P_{fail} , in the experiment together with the observed load level at cracking at the top surface and at the cross section edges of the slab are given in Table 1. To verify and validate the failure loads, comparison is made in the table with the yield lines solutions given in Eqs. (1)–(3) and the punching resistance according to EC2 from Eq. (6).

The main goal in this study was to study the bending behaviour of the slab. However, the ultimate capacity of the slab was governed by other failure mechanisms, like punching and anchoring or a combination of mechanisms, as seen in Table 1. In the slabs governed by punching a distinct cone was visible. An indication of anchoring problems was the observed horizontal cracks along the longitudinal reinforcement. The calculated yield line and punching capacities indicates a punching failure for the centre load and bending failure for edge and corner loads, which to a certain extent is confirmed in the tests.

Figure 8 shows the observed cracking at the top surface and the failure mechanism when the slab was loaded in the centre. Due to problems during testing, the slab was unloaded after reaching a load of 200 kN before starting loading again until failure. The failure mechanism at a load of 390 kN was a punching compression failure. The steel loading prism was pushed straight through the slab without any cracking close to the loading at the top surface. Only minor cracking was observed at the top

(a)



(b)



Figure 8. Crack patterns and failure for centre load [15].

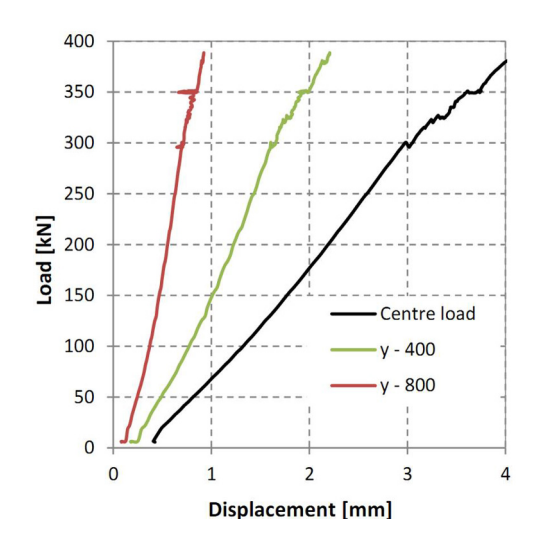
surface during loading, as seen in Figure 8. The first circular crack developed at a load of $320\ kN$ in a radial distance of $750\ mm$ from the loaded area.

The observed response of the slab subjected to a centre load is confirmed by the load-displacement and the strain development in Figure 9, where the notation y-400 e.g. means a measuring point 400 mm in y-direction from the centre of the loaded area. Locations of the strain and deformation measuring points and definition of the axes can be found in Figure 6. As expected the response is almost linear. Only the circular strain at the top surface, at a distance 800 mm from the loading area, shows a non-linear response after reaching a load of 300 kN. This is in agreement with the first top surface crack observed at a load level of 320 kN.

Figure 10 shows the crack patterns and failure mode of the concrete slab subjected to edge loading. The numbering on cracks corresponds to the load level in tonnes when the cracks were observed. As expected, circular cracks form at the top surface. The first crack occurred approximately

Table 1. Test results and calculated failure loads.

Load [kN]	Centre	Edge	Edge	Corner	Corner
	load	load 1	load 2	load 1	load 2
Crack top surface	325	80	85	33	30
Crack edge	-	35	40	40	40
P_{fail}	390	153	140	70	52
Failure type	punching	bending/	bending/	anchoring/	anchoring/
		punching	punching	bending	punching
P_{yield}	348	161	161	48	48
Ppunching	302	227	227	151	151



(b)

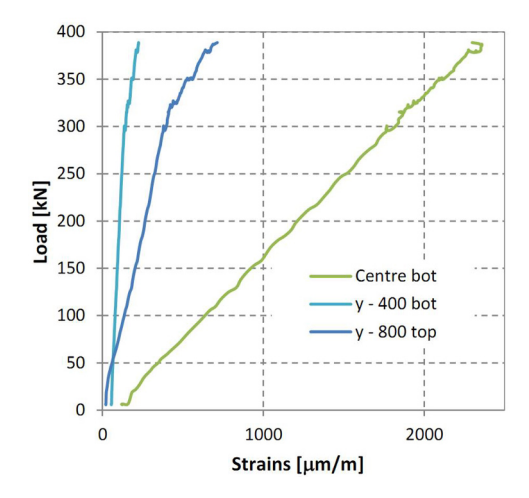


Figure 9. Centre load, (a) Displacements, (b) Strains.

500 mm from the edge towards the centre of the slab. With increasing loading, new cracks formed closer to the loading area. This is in accordance with redistribution of forces closer to the loaded area, as the slab starts to crack. The failure mechanism looks like a combination of a bending and a punching failure.

As seen from the load displacement graphs in Figure 11, the slabs has a non-linear response. The non-linearity is modest until approximately a load of $80\ kN$. This corresponds with the observed top surface cracking at the same load level.

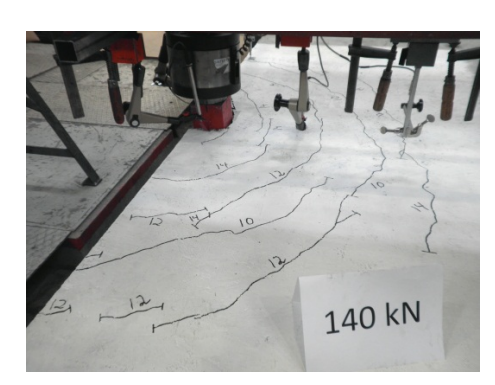
The strain development in Figure 11 for edge load 1 evidences the crack development in the slab. concentrated loading at the edge produces largest strains in the bottom side under the loaded area. The longitudinal strain along the slab edge at this point shows a pronounced increase at a load level of 30 kN (Figure 11). This is in agreement with the first observed crack at the edge at 35 kN. However, this is a very local effect which does not introduce a global non-linear behaviour in the slab, as seen from the strain development at other location points and the load-displacement graphs. Approaching a load of 80 kN, the circular strain placed at 649 mm towards the centre of the slabs, starts to show a nonlinear behaviour, which is in coincidence with the first visible crack at the top surface of the slab. With further increase in the load, more cracks form closer to the loaded area and along the edge.

The crack patterns and the failure mode for the two corner loads are presented in Figure 12. The top surface cracking started along the diagonal from the corner, at distances 440 (33 kN) and 340 mm (30 kN) for edge load 1 and 2 respectively, soon after the cracks extended to the corner edges. For corner load 1, two major cracks had formed at 40 kN. The failure at 70 kN was an anchoring failure initialised by the flexural cracking. The failure at 52 kN for corner load 2 was a combined punching/anchoring failure much closer to the loaded area than load 1, as seen in Figure 12.

(a)



(b)



(c)



(d)



Figure 10. Crack patterns at failure loads for edge loading [15], (a) Edge load 1, (b) Edge load 2, (c) Edge load 1, (d) Edge load 2

2 3 4
Displacement [mm]

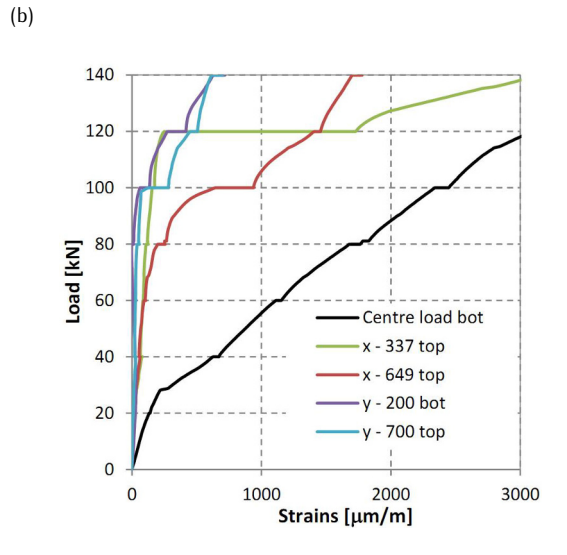


Figure 11. Edge load, (a) Displacements, (b) Strains.

The load-displacement graphs exhibited in Figure 13a, shows that corner load gives a local response. The radius of relative stiffness, *l*, for the slab, using the measured modulus of elasticity is 404 mm; at a distance of 1.0*l* from the loaded area, the deformation is halved. The strains in Figure 13b clearly indicate cracking at a load of approximately 35 kN, which corresponds to the observed cracking.







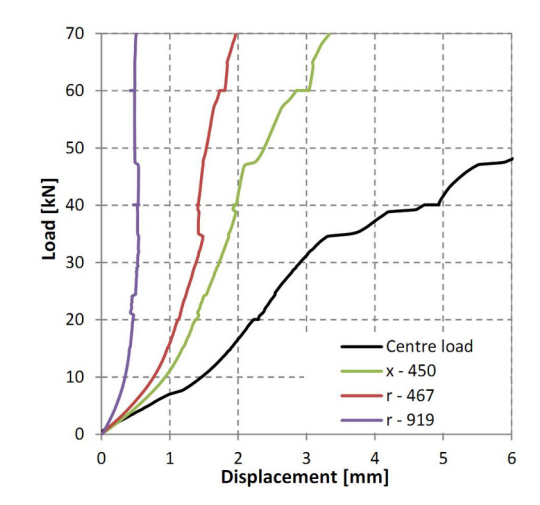
Figure 12. Crack patterns at failure for corner loading [15], (a) Corner load 1, (b) Corner load 2.

3. Numerical analysis

3.1. Model description

To verify and better understand the results from the tests described in Section 2, non-linear finite element analyses have been performed. The numerical analyses are carried out with the finite element code DIANA [18]. The focus in these analyses is on crack formations, deformations and global response in the slab. Hence, there is no tuning of material and numerical parameters to capture the mechanisms and the failure load. Often numerical analyses of slabs on ground focus on ultimate capacities and the influence of slab size and material parameters [19, 20]. Through a parametric study, the finite element model has been used to assess the influence of the tensile strength and the subgrade stiffness on the results. Drying shrinkage is often a major problem in concrete slabs, causing cracks on the top surface before





(b)

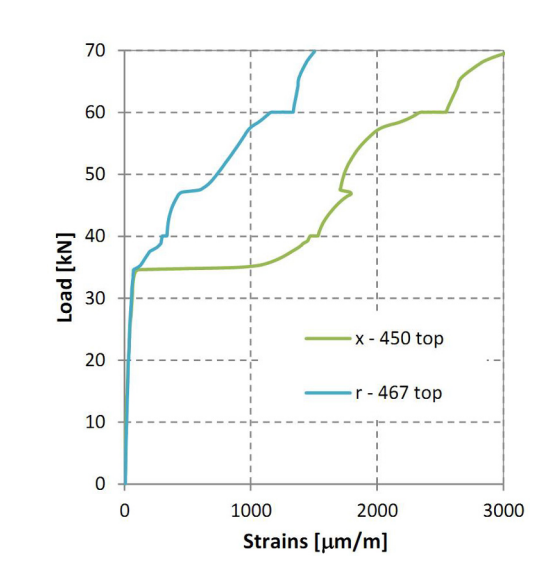


Figure 13. Corner load, (a) Displacements, (b) Strains.

any live loads are applied. Non-linear analyses are used to quantify the effect of shrinkage. Finite element analyses of slabs can use shell elements or solid elements. From a practical point of view, shell elements are preferred since the design of slabs is based on forces and moments which are the output from these elements. However, solid elements with stresses as output are able to model and analyse the response in more detail and with greater accuracy. Both element types have been employed in the analyses to see if shell elements give as good results as solid elements.

Two different finite element models have been

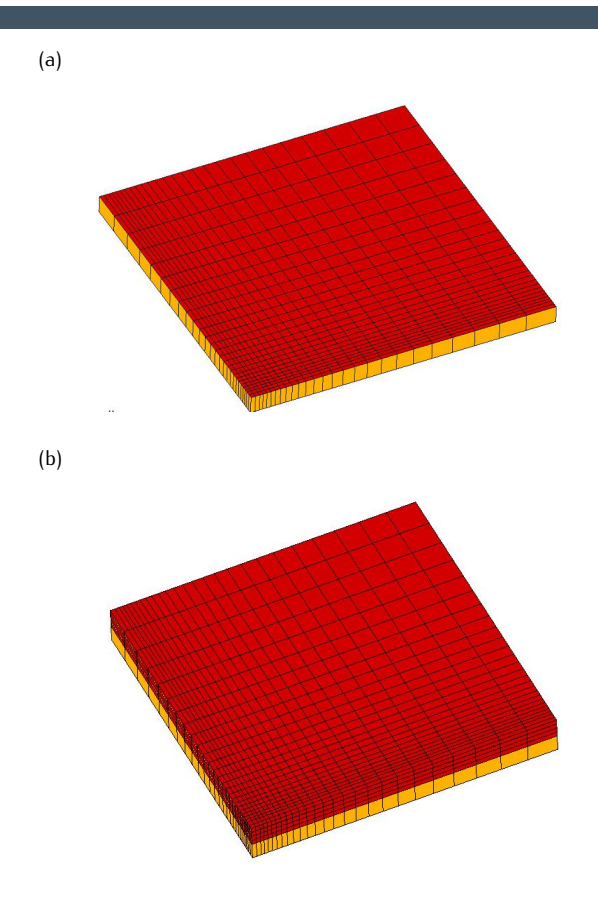


Figure 14. Finite Element models, (a) Shell elements, (b) Solid Elements.

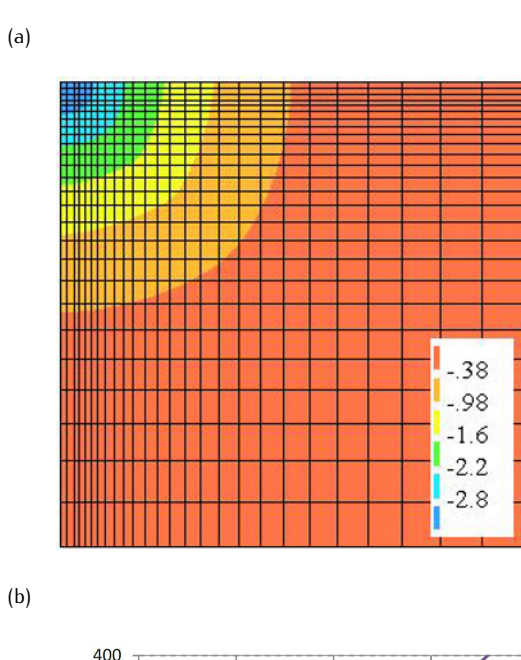
investigated. The first model employs three-dimensional quadratic shell elements with eight nodes. The second model consists of solid brick elements with 20 nodes with four elements over the cross section. To simulate the ground support, interface elements with eight nodes is used. Interface elements are capable of describing the relative vertical and tangential (horizontal) displacements between the concrete slab and the ground. Figure 14 shows the finite element models for the centre load with the interface elements at the bottom. Due to geometric symmetry, the finite element model represents only one quarter of the slab. Even though the concentrated loading from the experimental program described in Section 2 is not symmetric, this should not influence the result. The models in Figure 14 are also used for loading along the edge and at the corner. Only small adjustments of the mesh for edge and corner loads have been done to fit with the load area. Appropriate boundary conditions, depending on the location of the load, ensure the symmetry. The corner with the smallest element sizes is the loading area for all three loading situations.

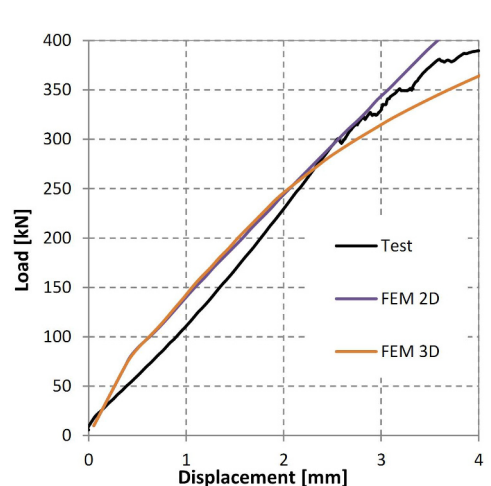
In order to simulate cracking, a smeared rotating crack model describes the tensile behaviour after reaching the tensile strength of 5.1 N/mm². After cracking, a linear tension softening model is utilised with an ultimate strain of 0.5% at zero tensile stress. Non-linear analyses of concrete subjected to concentrated loading often result in numerical instabilities and convergence problems due to high shear and compressive strains. Thus, concrete in compression is considered linear elastic since the focus in this study is on bending behaviour. The modulus of elasticity of the concrete is 26727 N/mm². The orthogonal reinforcement grid is modelled as embedded reinforcement and represented by a linear perfectly-plastic material model with yield strength of 564 N/mm². The constitutive model for the interface elements describes a no-tension bedding with a subgrade stiffness of 0.15 N/mm³ and zero friction. Hence, it takes into account the possible loss of contact between the slab and the soil, which simulates the experimental subgrade.

3.2. Numerical results

The simulated vertical slab displacement at the centre point is compared to the test results in Figure 15 for the centre load. Also, the contour plot of the displacement is given in the figure at a load level of 380 kN. As expected, the contour lines are almost perfect circular around the loaded area. The calculated and experimental results show reasonable match. The analyses have linear response up to a load level of approximately 80 kN, where non-linear response occurs. This corresponds well with the first observed crack in the analyses at the same load level. Before cracking, the simulated response is too stiff. The 2D and 3D results in Figure 15 represents the shell and the solid finite element model respectively. It can be observed that the models behave identical up to a load level of 250 kN; after that the 3D model has a more soft behaviour which is in better agreement with the test results.

In Figure 16 the crack pattern for the 3D model is presented at a load level of 380 kN. The pattern at the bottom is typical for slabs with centre loading. Crack bands form towards the outer edges and along the diagonal. The first crack occurred at 65 kN which explains the starting point of the non-linearity in the load versus displacement curve in Figure 15. The first registered top surface crack in the analysis was at 340 kN, which is in good accordance with the first observed crack at 325 kN in the test. As for the test, the numerical model shows only minor cracking at the top surface. This is in agreement with stress distribution in quadratic slabs. The highest stress concentrations are in areas between lines from the





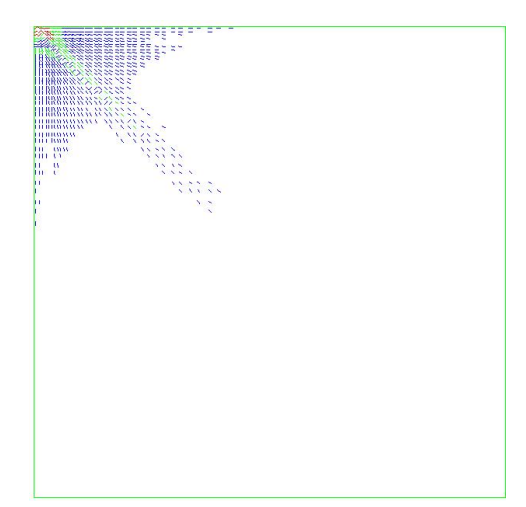


centre towards the edges and the diagonals, as it can be observed in the crack pattern of Figure 16.

Figure 17 shows the numerical vertical slab displacement below the edge load. The contour plot of the displacement in the figure corresponds to a load level of $140~\rm kN$. Compared to the circular contour lines for the centre load, the contour lines for the edge load is more oval shaped. This complies with distribution of forces in a ground slab subjected to an edge load. The sagging moments are larger and distributed wider along the free edge than towards the centre of the slab. The hogging moments are much larger towards the centre.

As seen in Figure 17, the response in the analyses is





(b)

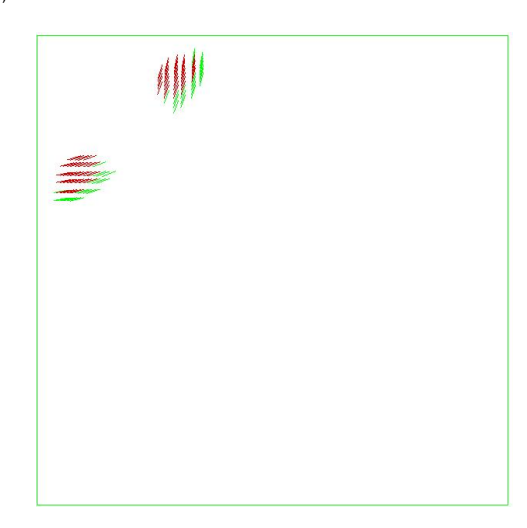
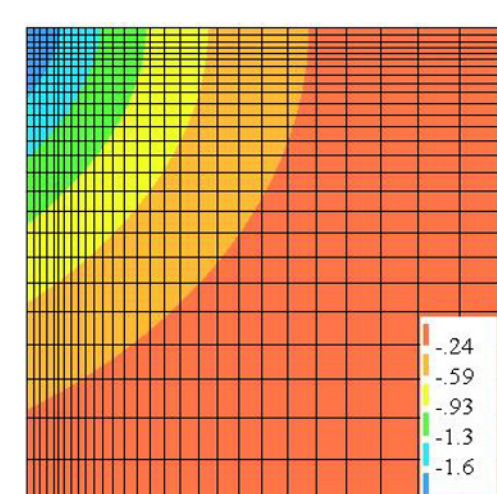


Figure 16. Crack pattern at 380 kN for centre load, (a) Bottom surface, (b) Top surface.

stiffer than the test. In the numerical analyses cracks occur at load levels of 25 kN and 90 kN for the bottom and top surface respectively. The shape of the displacement curves reflects this formation of cracks. Compared to the tests, the crack load at the bottom surface is very low. However, finite element modelling of concentrated loading yields very high stress gradients around the loaded area, which makes the results dependent on the element size. The 2D and 3D models behave identical up to a load level of 100 kN. Afterwards the 3D model has a more soft behaviour.

In Figure 18 the crack pattern at the top surface for the

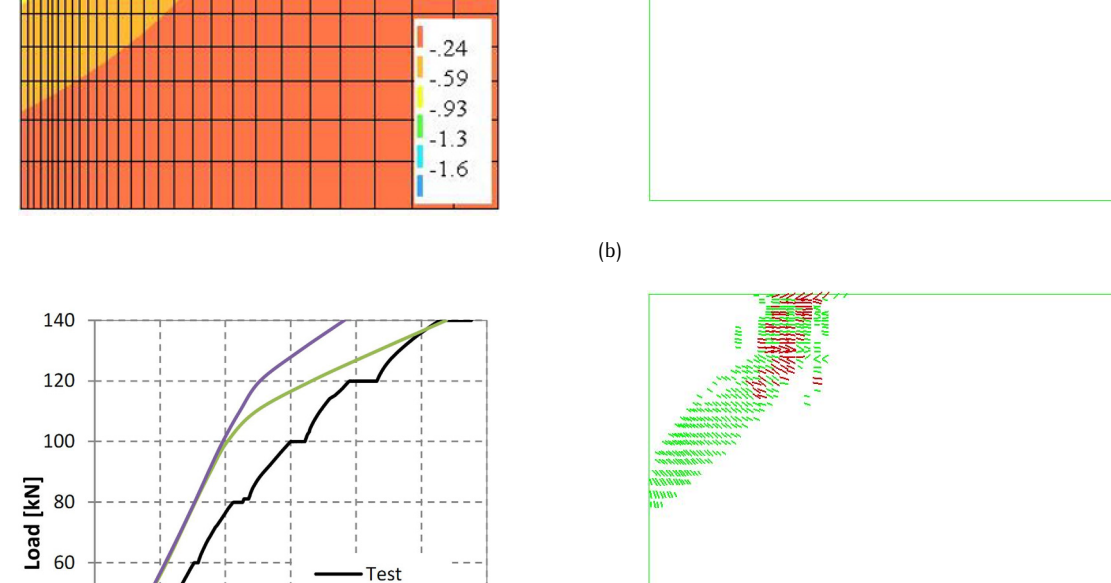


(b)

40

20

0 1



(a)

Figure 17. Edge load, (a) Vertical deformations [mm] at 100 kN, (b) Load-displacement curve.

Displacement [mm]

FEM 3D

FEM 2D

5

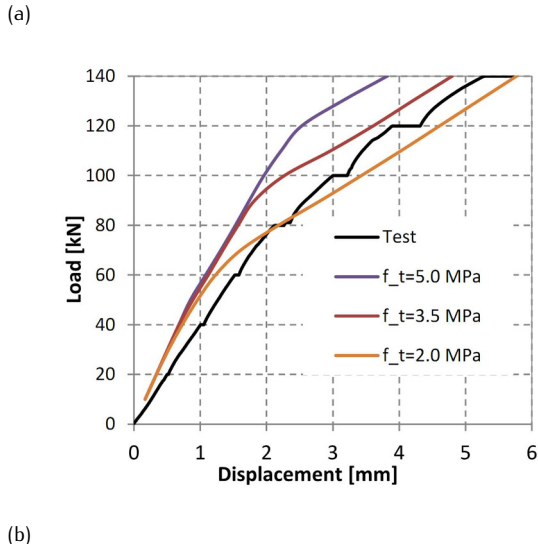
6

Figure 18. Crack pattern at top surface for edge load, (a) Load 100 kN, (b) Load 140 kN.

3D model is presented at load levels of 100 and 140 kN. The patterns describe the structural behaviour of the slab. At lower load levels, the large hogging moments towards the interior of the slab results in crack pattern seen in Figure 18a. Due to redistribution and higher loads, new cracks form further away from the loaded area along the free edge (Figure 18b). At the bottom surface, radial cracks will form mainly towards the interior of the slab.

The 2D finite element model has been used to assess the influence of the tensile strength and the subgrade stiffness on the results. As seen in Figure 19a, by lowering the tensile strength the numerical results are in better agreement with the test results. However, the response at low load levels is still too stiff. The subgrade stiffness is varied in Figure 19b; it can be observed that, with a stiffness of 0.10 N/mm³, the numerical and test results show reasonable match. The value of 0.15 N/mm³ used in these analyses is an average value based on test of the subgrade material. From Figure 4 it can be seen that the stiffness is lower than 0.15 N/mm³.

The simulated vertical slab displacement at the corner is compared to the test result in Figure 20 for the corner load. Also the contour plot of the displacement is given



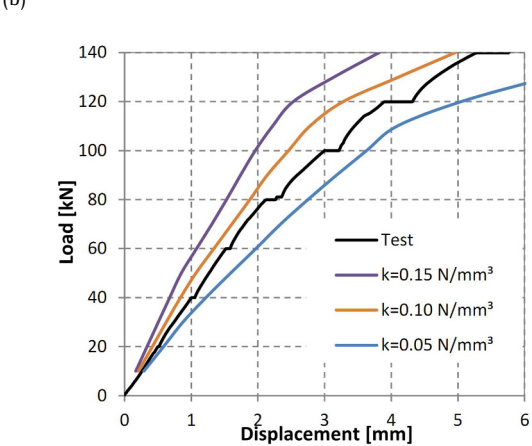
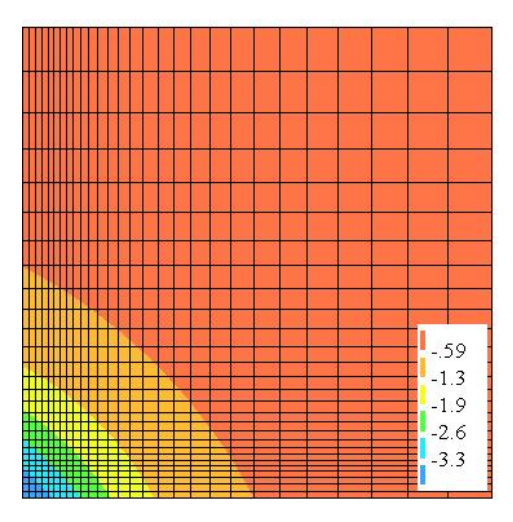


Figure 19. Edge load, effect of varying the (a) Tensile strength, (b) Subgrade stiffness.

in the figure at a load level of 40 kN. The contour lines are almost linear and divide the slab in triangles, which is typical for concentrated corner loads on ground supported slabs. The calculated and experimental results do not show very good match; the analyses have linear response up to a load level of approximately 40 kN, where a sudden and severe non-linear response occurs. This corresponds well with the extensive cracking in the analyses at the same load level. The numerical response is much too stiff before cracking; the test has a very soft and convex response for low load levels, while the numerical analyses with a constant subgrade stiffness of 0.15 N/mm³ is not capable of reproducing the experiments (Figure 20). The corner load gives very high support reactions in the subgrade. To see the effect of high support reactions and convex shape of the subgrade material, the non-linear





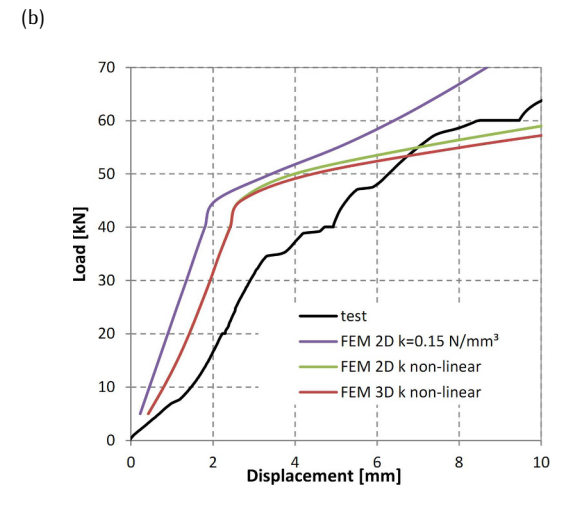
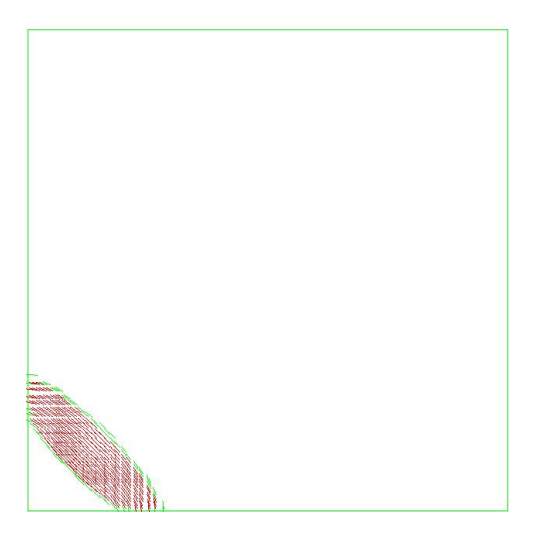


Figure 20. Corner load, (a) Crack pattern at top surface at 40 kN, (b) Distribution of stresses [N/mm²] in the top layer of reinforcement at 40 kN.

behaviour from Figure 4 is employed as the material model for the interface elements. The results in Figure 20 show a very small convexity and a softer response after cracking. However, the response is still too stiff at low loads. The results from the 2D and 3D models are almost identical, which is surprising since corner loading gives a very local response that solid elements should be able to predict better than shell elements.

In Figure 21a the crack pattern at the top surface for the 3D model is presented for a load of 40 kN. The crack band is very concentrated indicating there is one major crack in the analysis. This is confirmed with distribution of reinforcement stresses in the top layer in Figure 21b. The



(b)

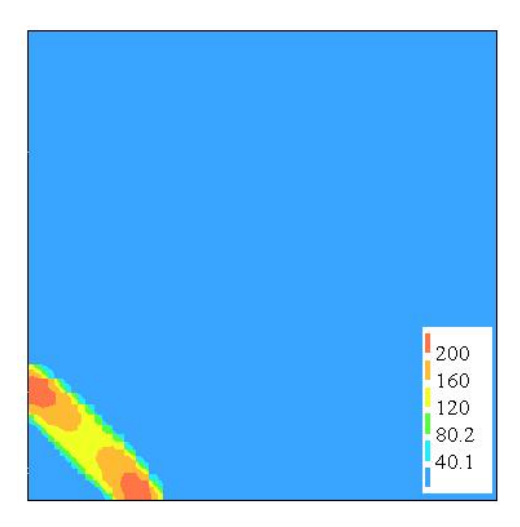


Figure 21. Corner load, (a) Crack pattern at top surface at 40 kN, (b) Distribution of stresses [N/mm²] in the top layer of reinforcement at 40 kN

centre of the cracking from the analysis is approximately 350 mm along the diagonal from corner, which is in the range of the test results.

3.3. Effect of shrinkage

Shrinkage can lead to significant tensile stresses in slabs on ground due to the one-side drying on the top surface. This can especially be a problem in areas with hogging moments, but even without any applied external load, top side cracking could occur. The effect of shrinkage

is often reported in experimental work and from practice, but is rarely taken into account in numerical analyses in the literature. In order to investigate the influence of shrinkage and to address the level of the tensile stresses, the 3D finite element model of a square slab from Section 3.1 is used together with a model for development if free shrinkage strain in a cross-section exposed to one-side drying.

A simplified solution of the diffusion equation for concrete exposed to drying is mainly characterized by the shrinkage penetration length, l_s , and the maximum free shrinkage strain ε_{cs0} [21]. If the penetration length is less than the cross-section height, the unrestrained shrinkage strain has a parabolic shape and yields:

$$\varepsilon_{cs} = \varepsilon_{cs0} \cdot \left(\frac{1 - y}{l_s}\right)^2$$

$$l_s = \sqrt{12 \cdot \alpha \cdot t}$$
(9)

where y is the distance from the drying surface, α is the diffusion coefficient and t the is the time in days. Only the effect of shrinkage after 28 days is considered. By assuming $\alpha=10~\text{mm}^2/\text{day}$, the penetration length is 58 mm. Thus, approximately, half the cross section is exposed to a parabolic distributed shrinkage strain in the numerical analysis. This study use 0.15‰as the maximum free shrinkage strain. The material properties related to shrinkage were not measured during the test program described in section 2. Thus, the effect of shrinkage on the test results cannot be quantified.

In order for shrinkage strains to cause stresses in a structure, there must be some kind of restraints from the geometrical shape or supports. In slabs on grade, the reaction forces from the ground introduce tensile stresses. However, if shrinkage is the only applied load together with a no-tension bedding material model for the ground, only minor stresses will appear due to the free lifting of the slab. Thus, in these analyses, the self-weight of the slab is applied together with the shrinkage strains. Two finite element models have been analysed. In the first model the outer edges of the slab is free to move vertically while the second model is supported to avoid vertical deformations at the edges. From Figure 22, it can be seen that the corner will lift more than 3 mm without the edge supports. Figure 23 presents the principal stress distribution at the top surface for both models. The obtained maximum tensile stresses are 3-4 N/mm², which is in the range of the tensile strength of concrete; hence, the slab may crack due to drying shrinkage. Large areas of the slabs have tensile stresses 1.5-3 N/mm², which is an indication on that drying shrinkage can be a problem and cause severe cracking in slabs on ground.

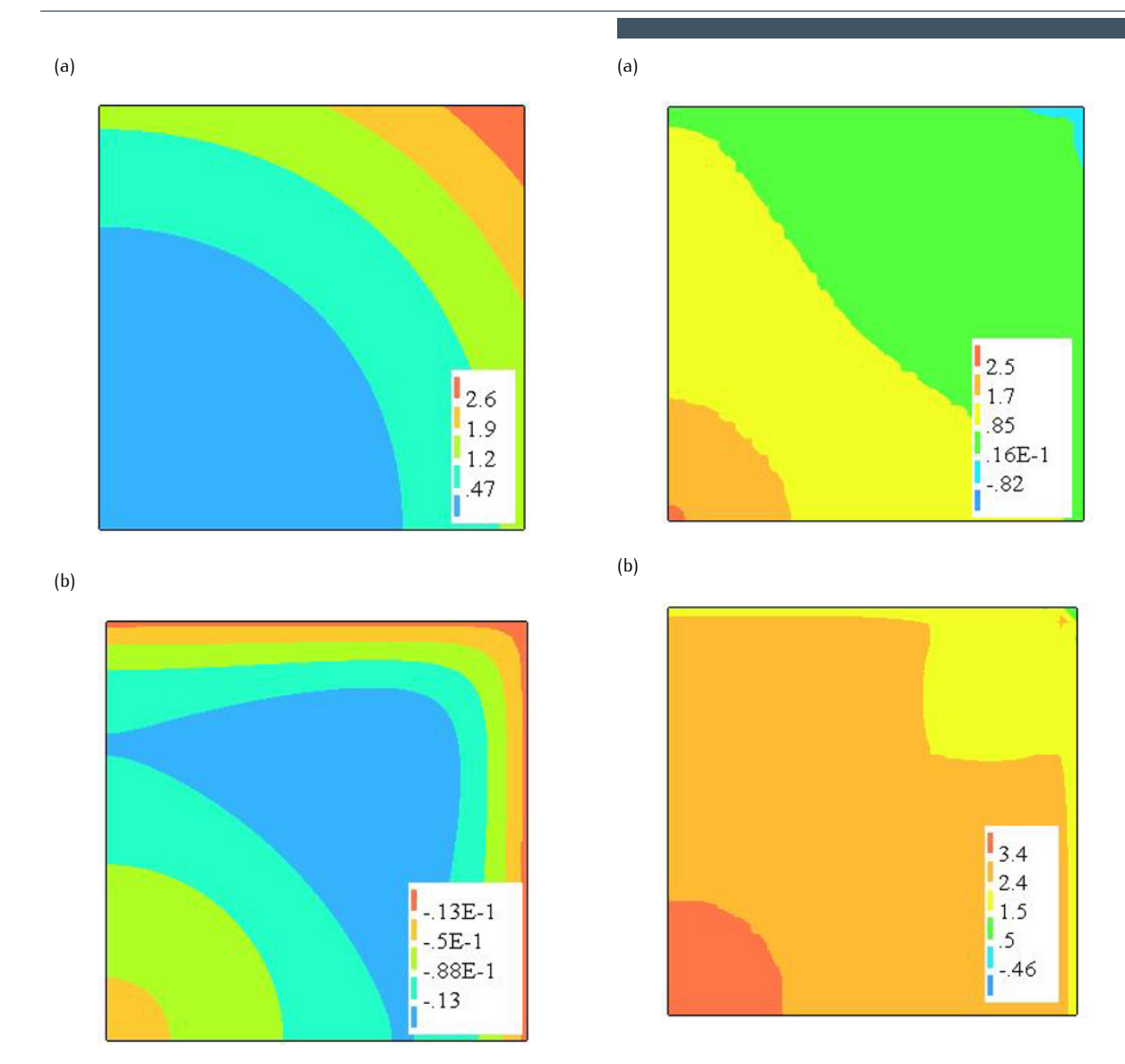


Figure 22. Distribution of vertical deformations [mm]: (a) Free boundaries, (b) Fixed boundaries.

Figure 23. Principal tensile stress at top surface [N/mm²], (a) Free boundaries, (b) Fixed boundaries.

Subgrade stiffness for typical grounds varies from $0.01~N/mm^3$ for fine sand to $0.5~N/mm^3$ for well compacted crushed stone. To investigate the effect of the stiffness on tensile stress due to shrinkage, the stiffness has been varied and compared with the obtained maximum principal tensile stress in the numerical analyses. The result presented in Figure 24 for the model with free edges indicates that typical values for the subgrade stiffness do not influence the tensile stresses very much.

4. Conclusions

In this study a concrete slab on grade was subjected to concentrated centre, edge and corner loads. The main goal was to study the formation of cracks on the top surface which often is of concern in this type of structure.

The response of the concrete slab was as expected; in fact, circular cracks formed at the top surface some distance away from the loading area, which is in agreement with linear elastic theory for slabs on elastic foundation. The failure mode was governed by punching for the centre load, a combined bending/punching for the edge load and anchoring/punching for the corner loads. The capacities

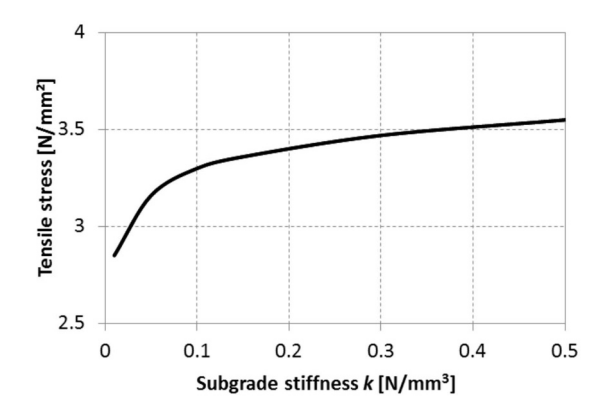


Figure 24. Effect of subgrade stiffness on the principal tensile stress.

were in agreement with requirements for punching in design codes and traditional yield line solutions for bending failures.

Non-linear finite element analyses were performed to verify the crack formation in the test program and to assess the influence of tensile strength and subgrade stiffness on the results. In general, the numerical analyses were able to predict first occurrences of cracks at the observed load levels and areas. However, the responses were too stiff for all three loading points. By reducing the subgrade stiffness, a better agreement was achieved between test and numerical results. Thus, to know the material characteristics of the grade is of great importance in this type of structure.

Slabs on grade are exposed to on-side drying which may cause tensile stresses at the top surface due to shrinkage. A numerical model which takes into account a time dependent strain profile in the cross-section was established. The results indicate that drying shrinkage can cause severe cracking in slabs on grade.

Acknowledgments

The author would like to gratefully acknowledge The Norwegian Concrete Association (Norsk Betongforening) for financial support to the experimental program and M.Sc Runar Heggem and M.Sc Frode Seglem for carrying out the experimental work.

References

- [1] Beckett D., Comparative tests on plain, fabric reinforced and steel reinforced concrete ground slabs, Concrete 24, 1990, 43–45
- [2] Falkner H., Huang Z., Teutsch M., Comparative study of plain and steel fiber reinforced concrete ground slabs, Concrete International 17, 1995, 45–51
- [3] Westergaard H. M., New formulas for stresses in concrete pavement of airfield, Transactions of ASCE 113, 1948, 425–444
- [4] Meyerhof G. G., Load-carrying capacity of concrete pavements, Journal of the Soil Mechanics and Foundations Division 88, 1962 89–116
- [5] Shentu, Jiang D., Hsu, Load-Carrying Capacity for Concrete Slabs on Grade, Journal of Structural Engineering 123, 1997, 95–103
- [6] Al-Nasra M., Wang L. R. L., Parametric study of slabon-grade problems due to initial warping and point loads, ACI Structural Journal 91, 1994, 198–210
- [7] Losberg A., Pavements and slabs on grade with structurally active reinforcement, ACI Journal Proceedings 75, 1978, 647–657
- [8] Rao K., Singh S., Concentrated LoadâĂŘCarrying Capacity of Concrete Slabs on Ground, Journal of Structural Engineering 112, 1986, 2628–2645
- [9] ACI, 360R-10. Guide for design of slabs-on-ground, American Concrete Institute, United States, 2010
- [10] Concrete Society, Concrete industrial ground floors: A quide to design and construction, 2003
- [11] Baumann R. R., Weisgerber F. E., Yield-Line analysis of slabs-on-grade, Journal of Structural Engineering 109, 1983, 1553–1568
- [12] Standards Norway, NS-EN 1992-1-1:2004+NA:2008. Eurocode 2: Design of concrete structures - General rules and rules for buildings, Standards Norway, Norway, 2008
- [13] CEB-FIP, Model code 1990, Thomas Telford, London, 1993
- [14] Knapton J., Ground bearing concrete slabs : specification, design, construction and behaviour, Thomas Telford, London, 2003
- [15] Heggen R., Seglem F., Ground bearing slabs subjected to concentrated loads, Master Thesis, Norwegian University of Science and Technology, Trondheim, Norway, 2010, (in Norwegian)
- [16] Standards Norway, NS-EN 12390-3:2009. Testing hardened concrete - Part 3: Compressive strength of test specimens Standards Norway, Norway, 2009
- [17] Standards Norway, NS 3676. Concrete testing - Hardened concrete - Modules of elasticity in compression, Standards Norway, Norway, 1987

- [18] TNO DIANA BV, DIANA Finite element analysis Release 9.4, The Netherlands, TNO DIANA BV, 2012
- [19] Alani A. M., Aboutalebi M., Analysis of the subgrade stiffness effect on the behaviour of ground-supported concrete slabs, Structural Concrete 13, 2012, 102– 108
- [20] Chou Y., Stress Analysis of Small Concrete Slabs
- on Grade, Journal of Transportation Engineering 110, 1984, 481–492
- [21] Planas J., Elices H., Shrinkage eigen stresses and structural size effect, In: Bazant Z.P. (Ed.), Fracture Mechanics of Concrete Structures, London: Elsevier; 1992